Bull. Fac. Bioresources, Mie Univ.
No.14 : 25−50
March 25. 1995

A Numerical Experiment on the Coastal Effects on the Western Boundary Current. Part I Effect of Inclined Coastline

Yoshihiko SEKINE and Akiya ASO
Faculy of Bioresources, Mie University

Abstract

Effect of coastal topography on the western boundary current is studied by use of a barotropic numerical model with special reference to the effect of inclination of the northern boundary from zonal direction. Detailed flow patterns of the numerical experiment are presented in this paper. It is resulted from the numerical experiment that there exists two representative flow pattern: one flow pattern is a meander flow and the other is a straight flow along northern boundary. In case of the meander flow pattern, spin-up and spin-down of the cyclonic eddy accompanied by meander flow are carried out. Meander flow pattern has a tendency to appear in the cases with zonal northern boundary. Chaotic change from meander pattern to straight flow pattern occurs in the case with the inclination of 10° and relatively small eddy viscosity. Straight flow pattern has a tendency to appear in the cases with the large inclination of the northern boundary from zonal direction.

1. Introducion

The Kuroshio, the western boundary current in North Pacific has a peculiar nature and shows bimodal path characteristics: a straight path and a large meander path[1-3]. Such large meander path is not observed in the Gulf Stream System and other western boundary currents[4]. The large meander in the Kuroshio has been studied by many investigators, and it has been shown that the large meander of the Kuroshio has a character of a stationary Rossby wave in the zonal flow and that the configuration of the coastal line is essential in dynamics of the Kuroshio meander[5-10]. The western boundary of the North Pacific Ocean is not straight and it runs rather zonally to the south of Japan. The Kuroshio flows almost eastward, and a Rossby wave can be easily generated there. In the present study, the coastline is simplified as shown in Fig. 1 and the coast south of Japan will be called as a northern coast for simplicity.

In early studies[5-8], it was argued that the Kuroshio takes large meander path when its volume transport and/or current velocity is relatively small while in later studies[11-14], that the Kuroshio takes the large meander path when the volume transport is relatively large. The difference between these two groups is whether inclusion of the effect of the north coast from the zonal direction is taken into account in the later studies or not taken into account in the early studies.

Sekine[12] examined the effect of the inclination of the north coast, and showed that the western boundary current is unstable and a meandering flow is formed when it flows zonally. In contrast, if the northern

coast inclines considerably from the zonal direction, the current is stable and flows in a straight path pattern along coast. In the previous paper[12], however, the northern coast in the meridional direction corresponding to the eastern coast of Honshu, Japan was not included in the model. In this paper, the effect of the inclination of the north coast will be examined further, including the northern coast in the model shown in Fig. 1.

2. Numerical model

A homogeneous ocean with a depth of 1000 m is assumed. We adopt a Cartesian coordinate system on a β plane with x-axis to east, y-axis to north. The vertically integrated equations under rigid lid approximation and hydrostatic balance are transformed into the vorticity equation:

$$\frac{\partial z}{\partial t} = -\frac{\partial uz}{\partial x} - \frac{\partial vz}{\partial y} - \beta v + A_h \nabla^2 z, \qquad (1)$$

$$z = \frac{\partial v}{\partial x} - \frac{\partial u}{\partial y} = \frac{\partial}{\partial x}\left(\frac{1}{h}\frac{\partial \phi}{\partial x}\right) + \frac{\partial}{\partial y}\left(\frac{1}{h}\frac{\partial \phi}{\partial y}\right). \qquad (2)$$

The symbols used in the above equations are tabulated in Table 1. The system is driven by in- and outflow with a volume transport of 55 Sv (1 Sv = 10^{12} cm^3 sec^{-1}). Inflow is given at the southern boundary and outflow at the eastern boundary. Sinusoidal horizontal velocity distribution of the in- and outflow is assumed and only northward velocity component is given at the southern open boundary:

$$\phi = \phi_0 - \phi_0 \cos(\pi x / L_i) \quad \text{for } 0 \leqq x \leqq L_i \qquad (3-1),$$

$$\phi = 2\phi_0 \quad \text{for } L_i \leqq x \qquad (3-2),$$

where ϕ_0 is a half of the total transport of the in- and outflow and L_i (=187 km) is the width of the inflow (Fig. 1). The Similar boundary condition is imposed at the eastern outflow boundary.

$$\phi = 2\phi_0 \quad \text{for} \quad 0 \leqq y \leqq 1020.5 \text{ km} \qquad (4-1),$$

$$\phi = \phi_0 - \phi_0 \cos(\pi (y - 1020.5)/Lo) \quad \text{for} \quad 1020.5 \text{ km} \leqq y \qquad (4-2),$$

where Lo (=157 km) is the width of the outflow. Viscous boundary condition is imposed on the northern boundary and slip condition is imposed on the others boundaris. In the numerical calculation, we adopt a rectangular grid with horizontal spacing of 18.7 km in west-east direction and 15.7 km in southnorth direction.

In the present study, eight cases of numerical experiments with different model character are performed (Table 2). Firstly, a relatively small eddy viscosity with $A_h = 5 \times 10^6$ cm^2 sec^{-1} is assumed and coastal topographic effect is examined by use of four models with different inclination of northern

boundary from zonal direction (Fig. 1). Models with the inclination from zonal direction (θ in Fig. 1) with 0°, 10°, 20° and 30° are referred to as V00SE, V10SE, V20SE and V30SE, respectively (Table, 2). Secondly, similar four experiments are performed assuming relatively large eddy viscosity with $A_h = 1\times10^7 cm^2sec^{-1}$, of which four models with the similar inclination of the northern boundary from zonal direction are referred to as V00LE, V10LE, V20LE, and V30LE, respectively.

Table 1 List of symbols

t	: time
x	: eastward component of Cartesian coordinate
y	: northward component of Cartesian coordinate
u	: x-directed (eastward) component of horizontal velocity
v	: y-directed (northward) component of horizontal velocity
d	: depth of the ocean
z	: relative vorticity
ϕ	: volume transport function
β	: linear change rate of the Coriolis parameter ($\beta = 2 \times 10^{-13} cm^{-1} sec^{-1}$)
A_h	: coefficient of horizontal eddy viscosity
∇^2	: Laplacian operator for the horizontal direction

Table 2 Parameters of the experiments

Run	Inclination of northern coastal boundary (θ in Fig. 1) (in degree)	Coeffient of horizontal eddy viscosity (A_h) (in cm^2sec^{-1})
V00SE	0	5×10^6
V10SE	10	5×10^6
V20SE	20	5×10^6
V30SE	30	5×10^6
V00LE	0	1×10^7
V10LE	10	1×10^7
V20LE	20	1×10^7
V30LE	30	1×10^7

3. Results

3 − 1 Cases with zonal northern boundary ($\theta = 0°$)

The result of V00SE with relatively small eddy viscosity ($A_h = 5 \times 10^6 cm^2 sec^{-1}$) is shown in Fig. 2. An anti-cyclonic and a cyclonic eddy are formed in a northwestern area and a mean flow shows a large meander pattern. The cyclonic eddy is weakened and stretched in southward direction. Later, this cyclonic eddy is cut-off from the mean flow and decays at about 55 days. However, very small cyclonic area remains near the northern boundary and a new cyclonic eddy is generated in eastern area. This cyclonic eddy shifts westward and develops furthermore in the northwestern area. The flow pattern at 90 days resembles to that of 40 days and similar decay of the cyclonic eddy to that in 50 ~ 60 days is carried out in 120 ~ 125 days. In later time, similar spin-up and spin-down are repeated (Fig. 2). Namely, the former corresponds to the formation of cyclonic eddy and development of the cyclonic eddy through eastward shift, the latter is the decay of the cyclonic eddy after its cut-off from the mean flow.

In order to see the details of the time evolution of the cyclonic eddy, time change in the volume transport of the cyclonic eddy is shown in Fig. 3 a. The spin-up and spin-down of the cyclonic eddy has a periods of 70 days. Small variation is detected after the occurrence of the spin-up shown by the abrupt increase

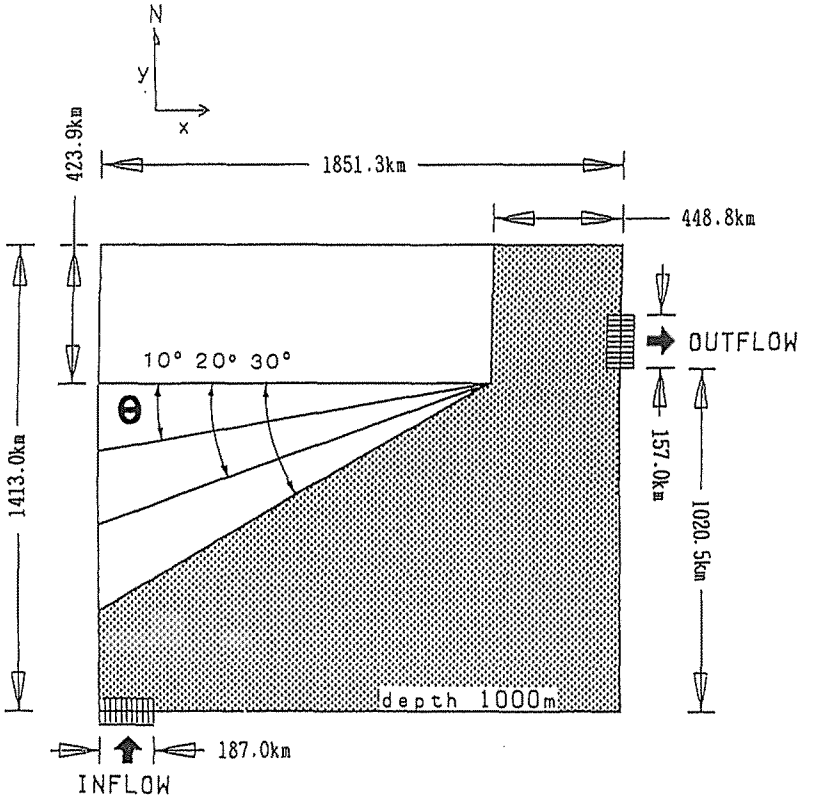

Fig. 1 Schematic view of the numerical model with four different northern coastal bound-aries. Two hatched area with closed arrows indicate the boundary with in- and

Fig. 2－1

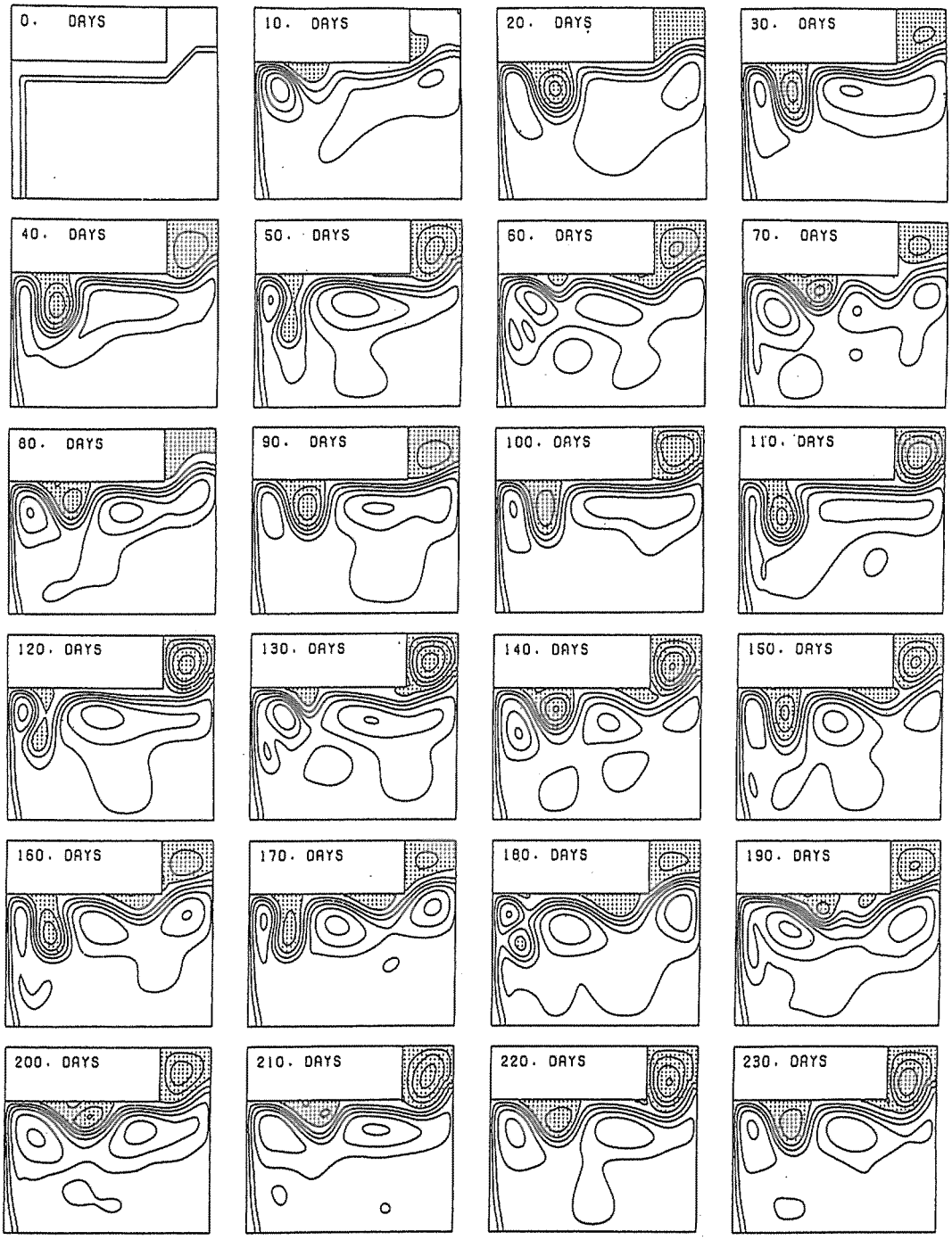

Fig. 2 Results of V00SE shown by the spatial distribution of volume transport function. The contour interval of transport function is 20 Sv and areas with negative volume transport function are stippled.

Fig. 2 – 2

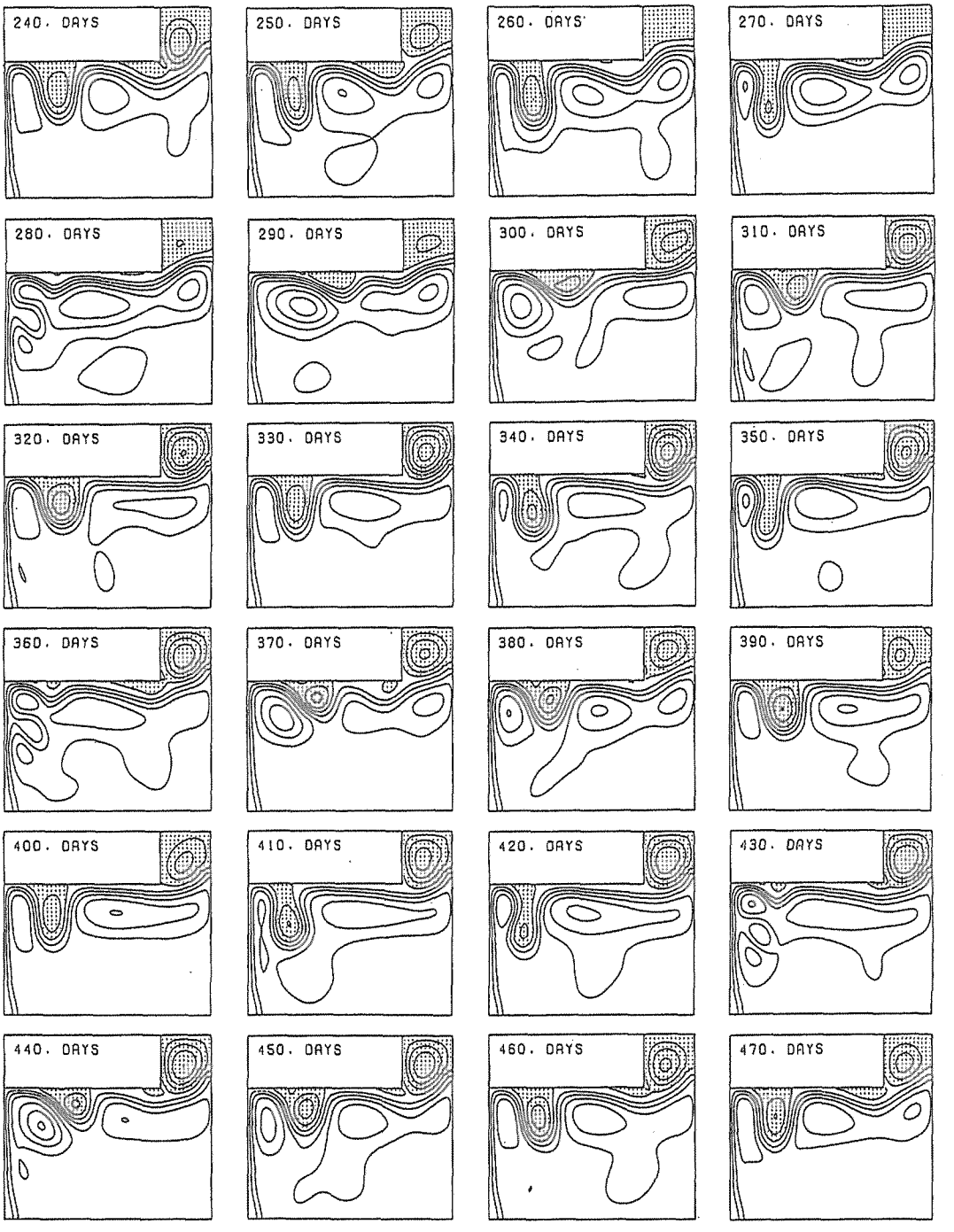
240. DAYS
250. DAYS
260. DAYS
270. DAYS
280. DAYS
290. DAYS
300. DAYS
310. DAYS
320. DAYS
330. DAYS
340. DAYS
350. DAYS
360. DAYS
370. DAYS
380. DAYS
390. DAYS
400. DAYS
410. DAYS
420. DAYS
430. DAYS
440. DAYS
450. DAYS
460. DAYS
470. DAYS

Fig. 2 – 3

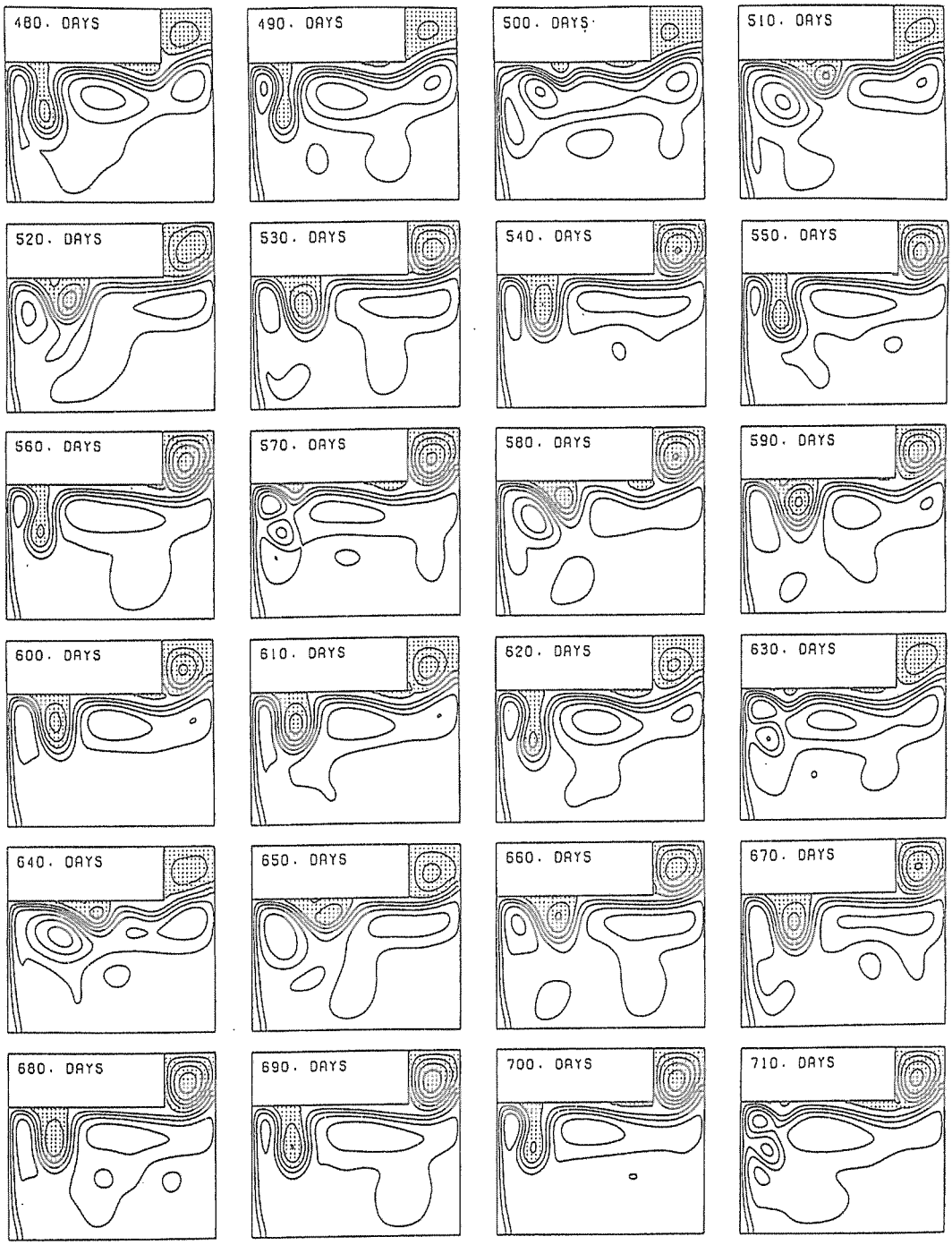
480. DAYS
490. DAYS
500. DAYS
510. DAYS
520. DAYS
530. DAYS
540. DAYS
550. DAYS
560. DAYS
570. DAYS
580. DAYS
590. DAYS
600. DAYS
610. DAYS
620. DAYS
630. DAYS
640. DAYS
650. DAYS
660. DAYS
670. DAYS
680. DAYS
690. DAYS
700. DAYS
710. DAYS

in the volume transport of the cyclonic eddy. These correspond to the enhancement of the cyclonic eddy during the westward shift and just before the cut-off from the mean flow. The former case is seen in the flow patterns in 380 - 390 days and 580 - 590 days, the latter in 400 - 410 days and 680 - 690 days.

The result of V00LE with relatively large eddy viscosity ($A_h = 10^7 cm^2 sec^{-1}$) is shown in Fig. 4. The spin-up and spin-down of the cyclonic eddy are also carried out. However, some different patterns from V00SE are detected. Firstly, there exists a decrease in the period of the spin-up and spin-down : the first decay of the cyclonic eddy occurs spin-up in 40 days, while that in V00SE occurs at 55 days, which is clear in the time change in the volume transport of the cyclonic eddy shown in Fig. 5 a. It is shown that the averaged period of the spin-up and spin-down is about 50 days over all the time integrated period of 1000 days, while that of V00SE is 70 days (Fig. 3 a). Another difference is no enhancement of the cyclonic eddy, which is detected in the flow pattern of 30 - 40 days. Furthermore, cut-off of the cyclonic eddy is not carried out. The cyclonic eddy monotonously decays after elongating southward. On the whole, it is demonstrated that a large frictional effect in V00LE enhances the decay of the cyclonic eddy in comparison with that in V00SE and it results in the short period of spin-up and spin-down and no occurrence of the spin-up and the cut-off of the cyclonic eddy.

3 − 2 Cases with inclined northern boundary ($\theta = 10°$)

The result of V10SE with the small eddy viscosity is shown in Fig. 6. A cyclonic eddy is formed and its volume transport oscillates around 40 Sv (Fig. 3 b). After the southward elongation at about 110 days, cut-off is carried out in 120-130 days and the cut-off eddy decays in 135 days. However, remaining cyclonic eddy near the northern boundary is maintained and enhanced again after 140 days. This

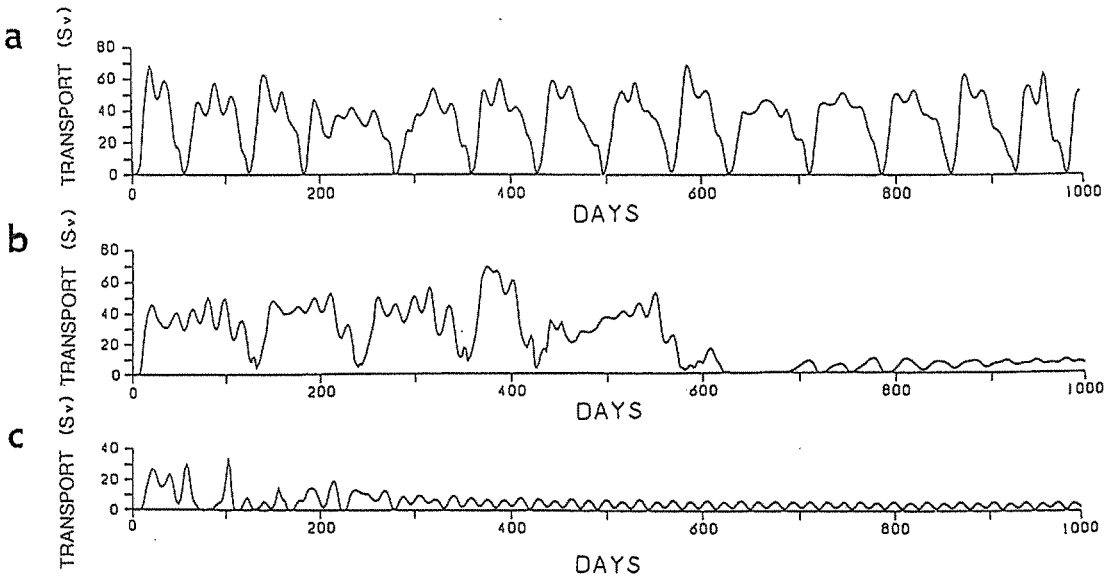

Fig. 3 Time change in the volume transport of the cyclonic eddy. (a) V00SE, (b) V10SE and (c) V20SE.

Fig. 4 – 1

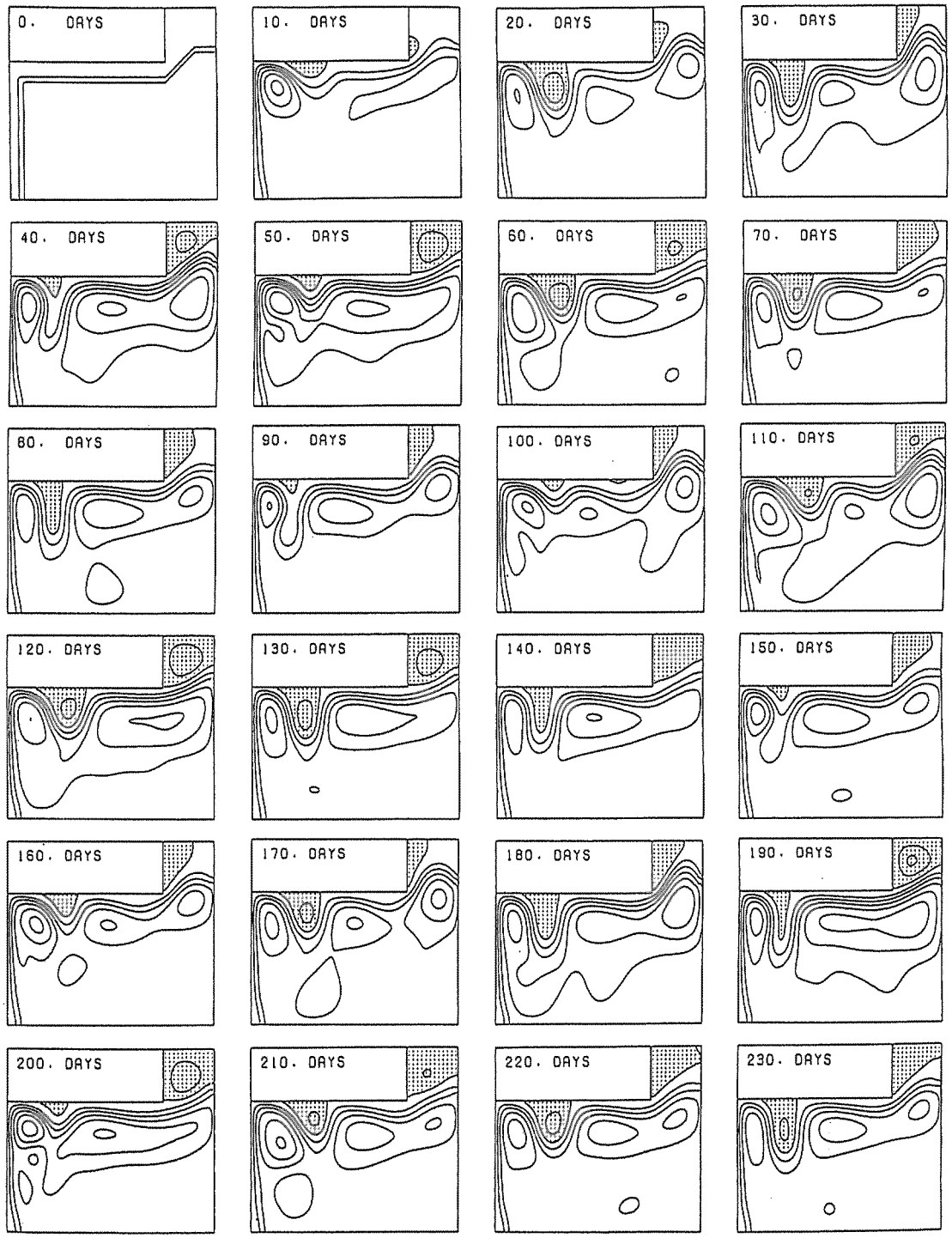

Fig. 4 Same as in Fig. 2, but for V00LE.

Fig. 4 – 2

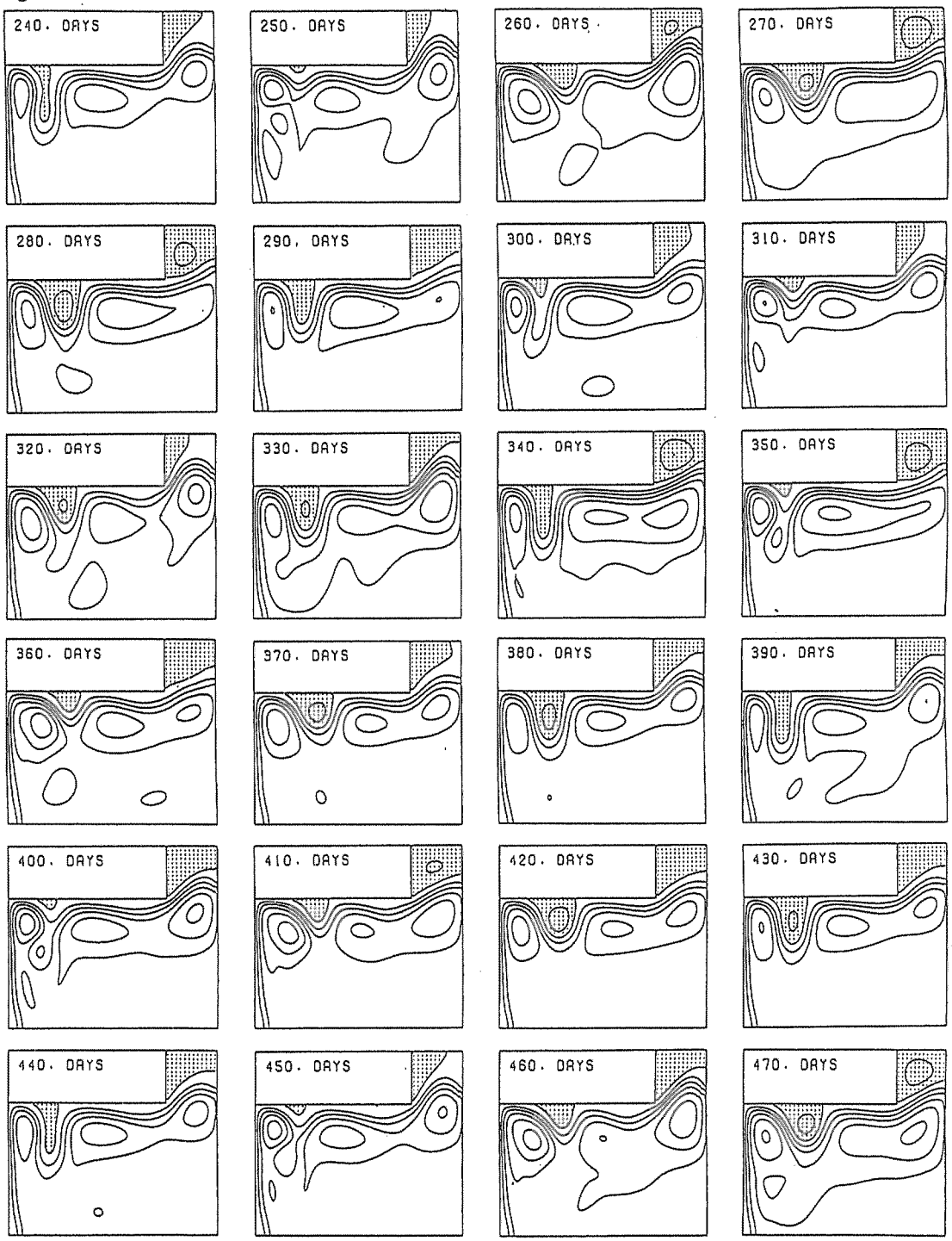
240. DAYS
250. DAYS
260. DAYS
270. DAYS
280. DAYS
290. DAYS
300. DAYS
310. DAYS
320. DAYS
330. DAYS
340. DAYS
350. DAYS
360. DAYS
370. DAYS
380. DAYS
390. DAYS
400. DAYS
410. DAYS
420. DAYS
430. DAYS
440. DAYS
450. DAYS
460. DAYS
470. DAYS

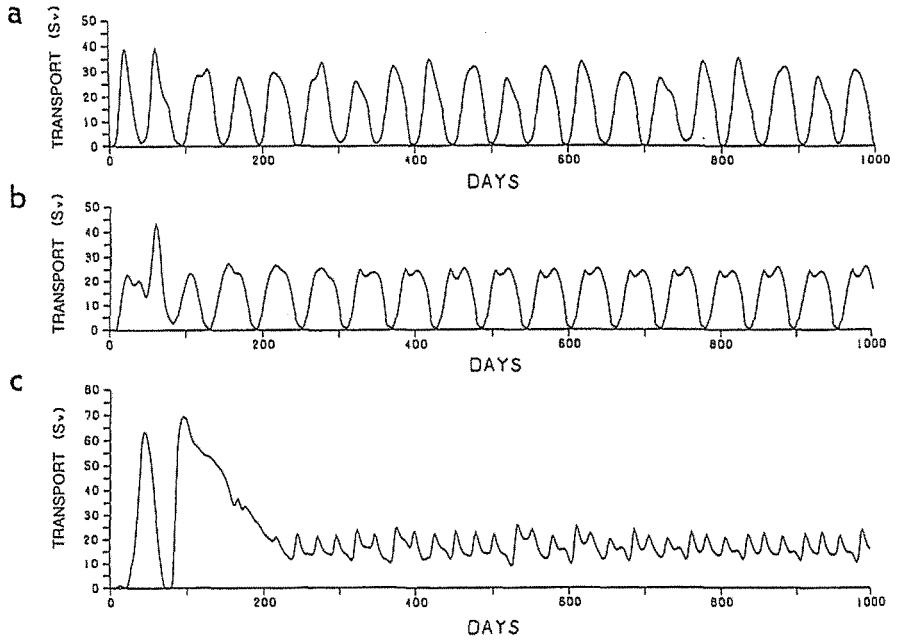

Fig. 5 Same as in Fig. 3, but for the cases with larger eddy viscosity. (a) V00SE, (b) V10SE and (c) V20SE.

cyclonic eddy is elongated southward at 220 days and decays at 245 days. The spin-up and spin-down of the cyclonic eddy are repeated upto 580 days. However, it should be noticed that the spin-up of the cyclonic eddy does not occurs afterwards and only large anti-cyclonic circulation is formed. This anti-cyclonic circulation is stables and the straight flow along northern boundary is maintained stationary. On the whole, it is suggested that there exist two representative flow patterns in this model. One is a meander flow patten and other one is a straight flow along northern boundary.

The results of V10LE with the larger eddy viscosity is shown in Fig. 7. Although growth of the cyclonic eddy is almost common to V10SE, the spin-down occurs quickly: the first decay of the cyclonic eddy occurs at about 90 days, while the decay in V10SE occurs at about 135 days. After this, almost similar spin-up and spin-down are repeated (Fig. 5b). Thus, the straight mean flow shown in V10SE (Fig. 6) is not formed in this case.

3 − 3 Cases with inclined northern boundary ($\theta = 20°$)

Results of V20SE are shown in Fig. 8. A cyclonic eddy is formed in the eastern area of the northern boundary and it does not show the westward shift. This cyclonic eddy decays at 120 days and a dominant anti-cyclonic circulation is generated in the central basin. The total flow pattern resembles to that of V10SE in the later period. Because of the southwestward intrusion of the cyclonic eddy, mean flow separates from the northern boundary.

Results of V20LE are shown in Fig. 9. Almost similar flow patterns to those of V20SE are found in the initial stage, however development of the two cyclonic eddies is relatively slow. In particular, southwestward intrusion of the cyclonic eddy does not occur and the separation of the mean flow is not

Fig. 6 – 1

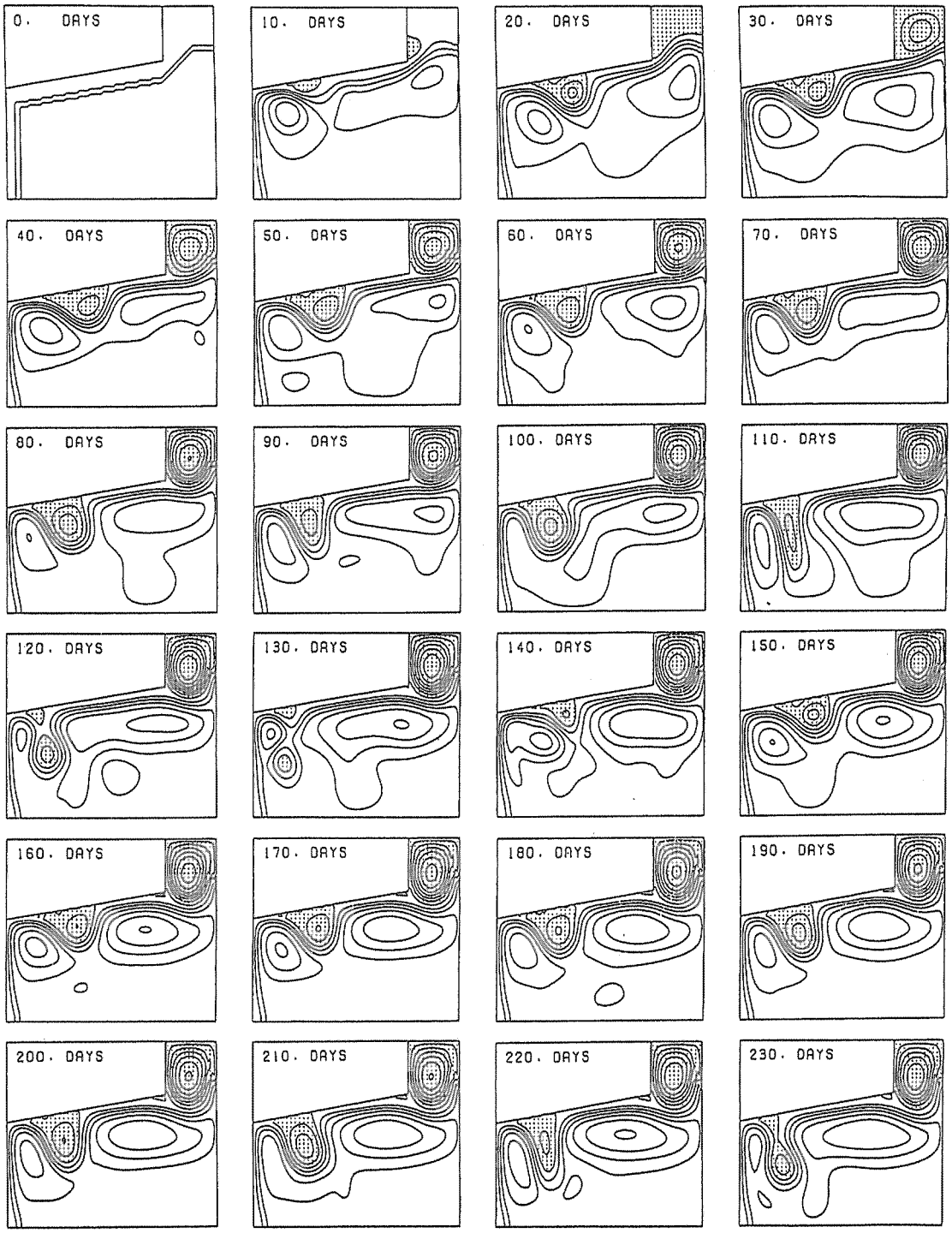

Fig. 6 Same as in Fig. 2, but for V10SE.

Fig. 6 – 2

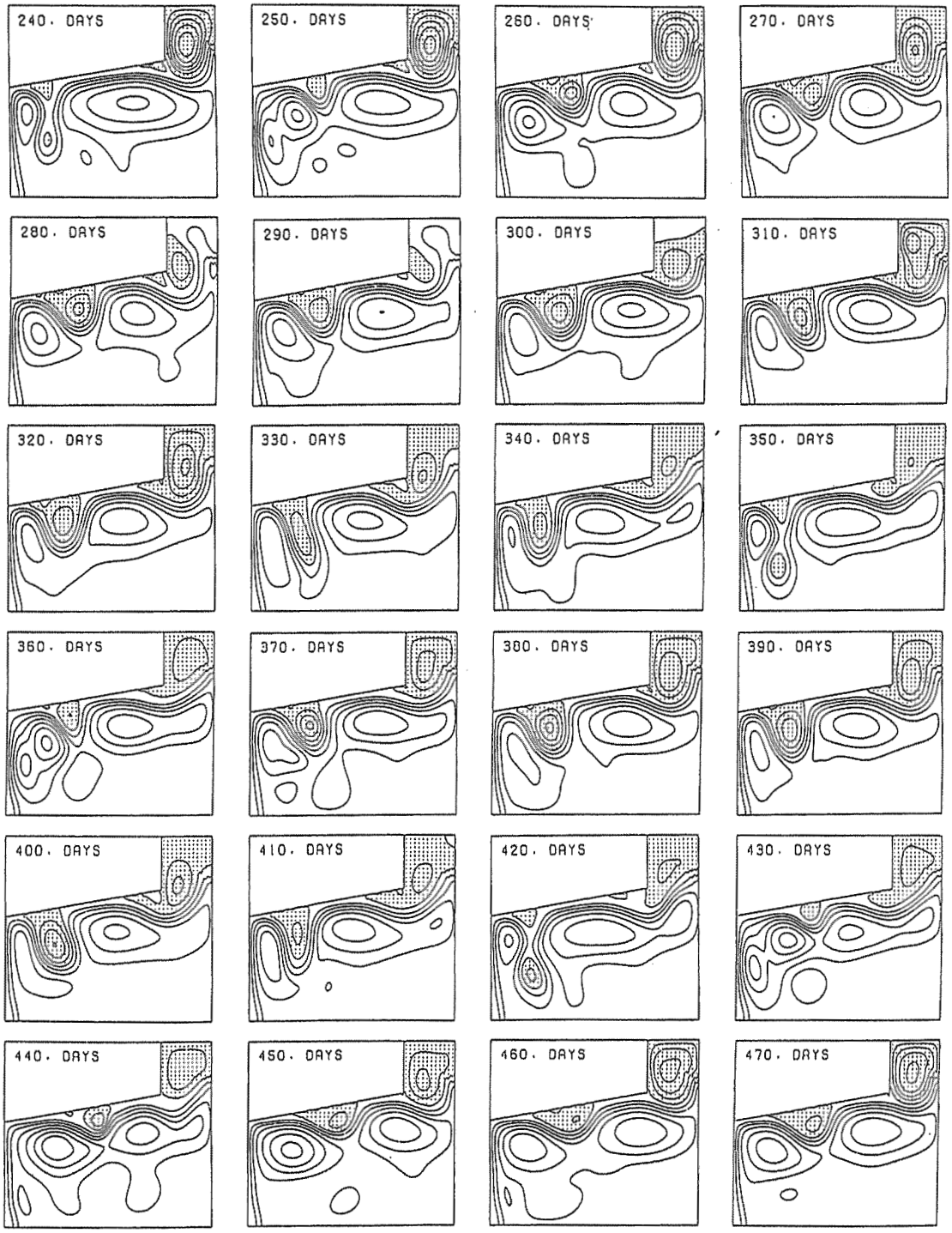
240. DAYS
250. DAYS
260. DAYS
270. DAYS
280. DAYS
290. DAYS
300. DAYS
310. DAYS
320. DAYS
330. DAYS
340. DAYS
350. DAYS
360. DAYS
370. DAYS
380. DAYS
390. DAYS
400. DAYS
410. DAYS
420. DAYS
430. DAYS
440. DAYS
450. DAYS
460. DAYS
470. DAYS

Fig. 6 – 3

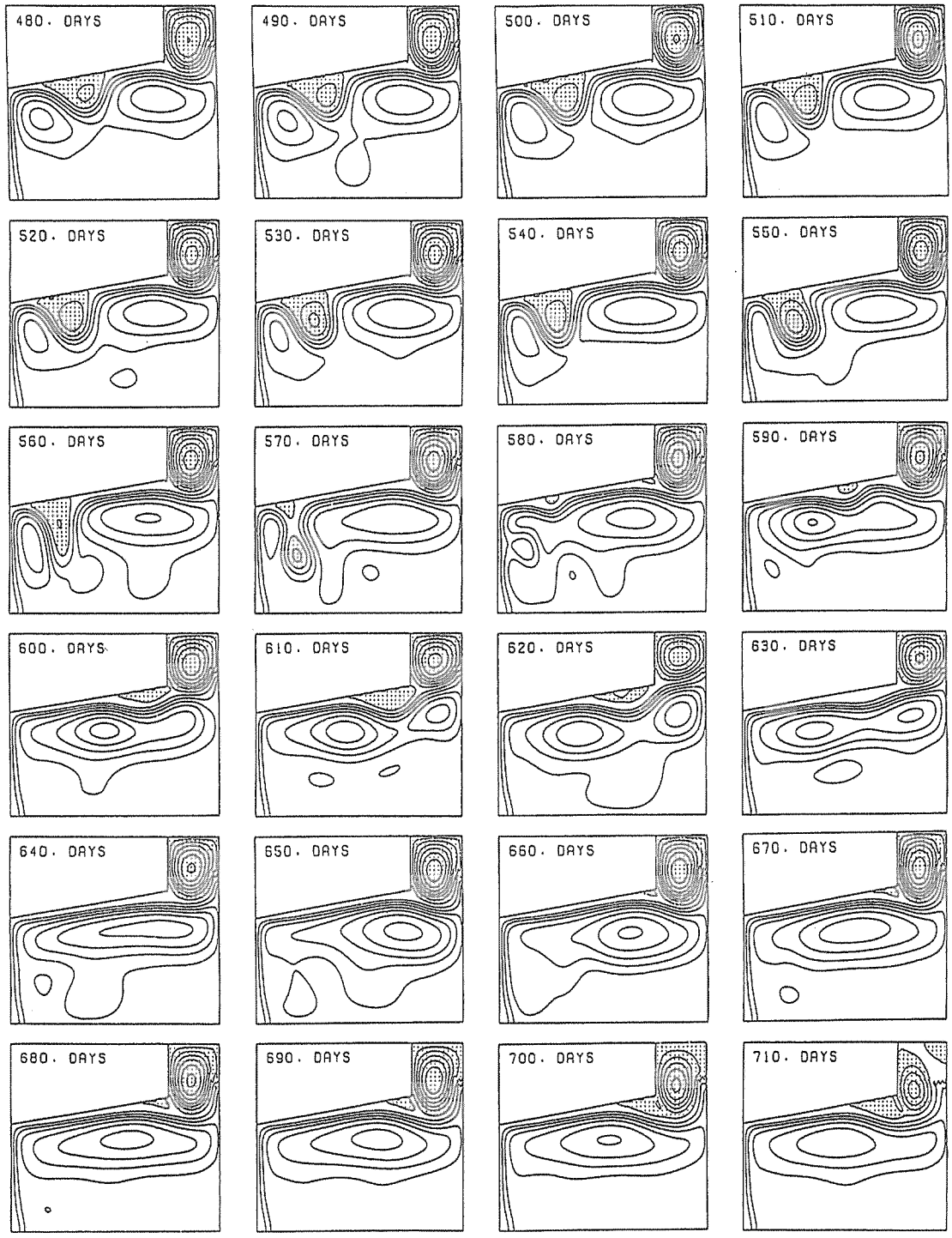
480. DAYS
490. DAYS
500. DAYS
510. DAYS
520. DAYS
530. DAYS
540. DAYS
550. DAYS
560. DAYS
570. DAYS
580. DAYS
590. DAYS
600. DAYS
610. DAYS
620. DAYS
630. DAYS
640. DAYS
650. DAYS
660. DAYS
670. DAYS
680. DAYS
690. DAYS
700. DAYS
710. DAYS

Fig. 6 – 4

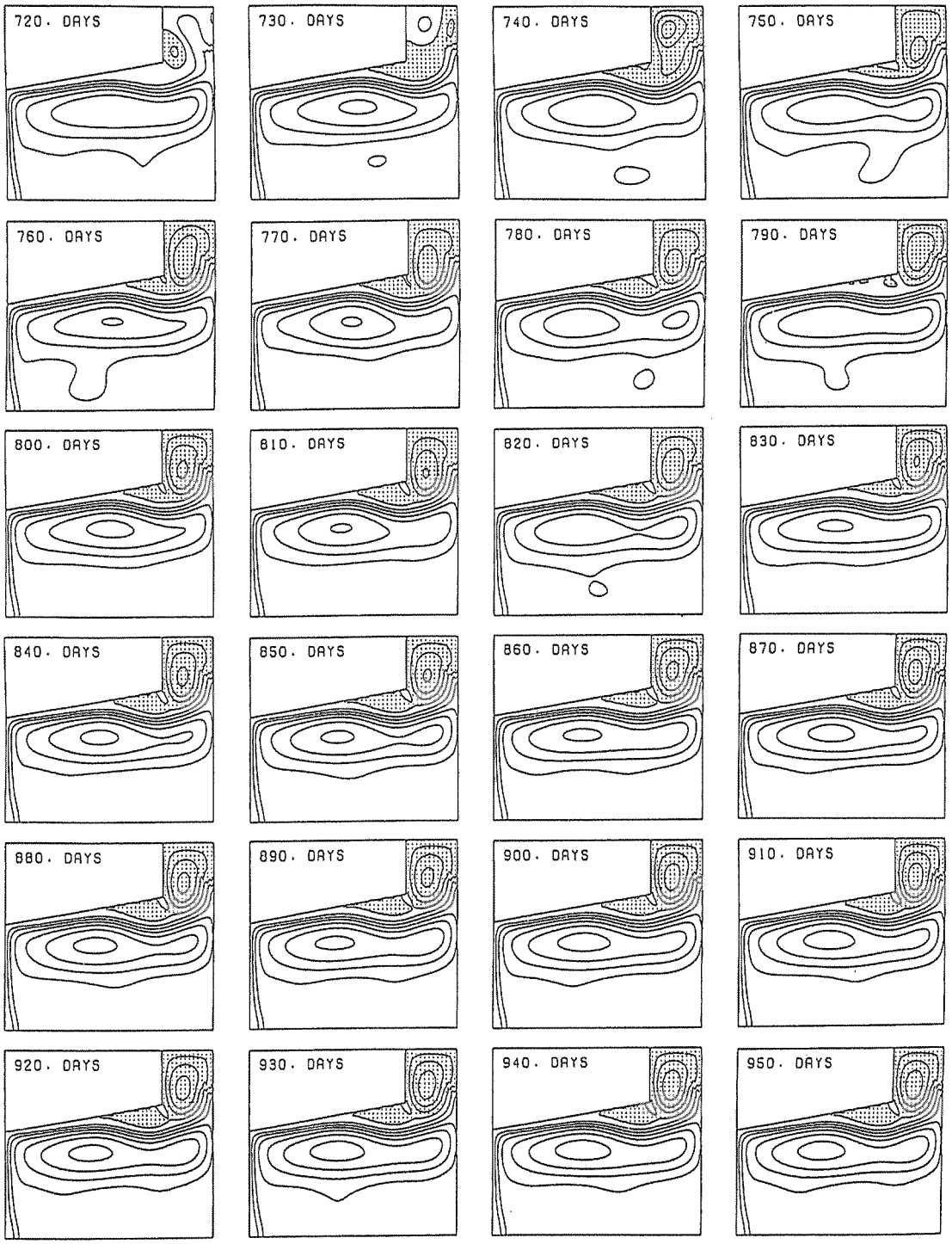
720. DAYS
730. DAYS
740. DAYS
750. DAYS
760. DAYS
770. DAYS
780. DAYS
790. DAYS
800. DAYS
810. DAYS
820. DAYS
830. DAYS
840. DAYS
850. DAYS
860. DAYS
870. DAYS
880. DAYS
890. DAYS
900. DAYS
910. DAYS
920. DAYS
930. DAYS
940. DAYS
950. DAYS

Fig. 7 – 1

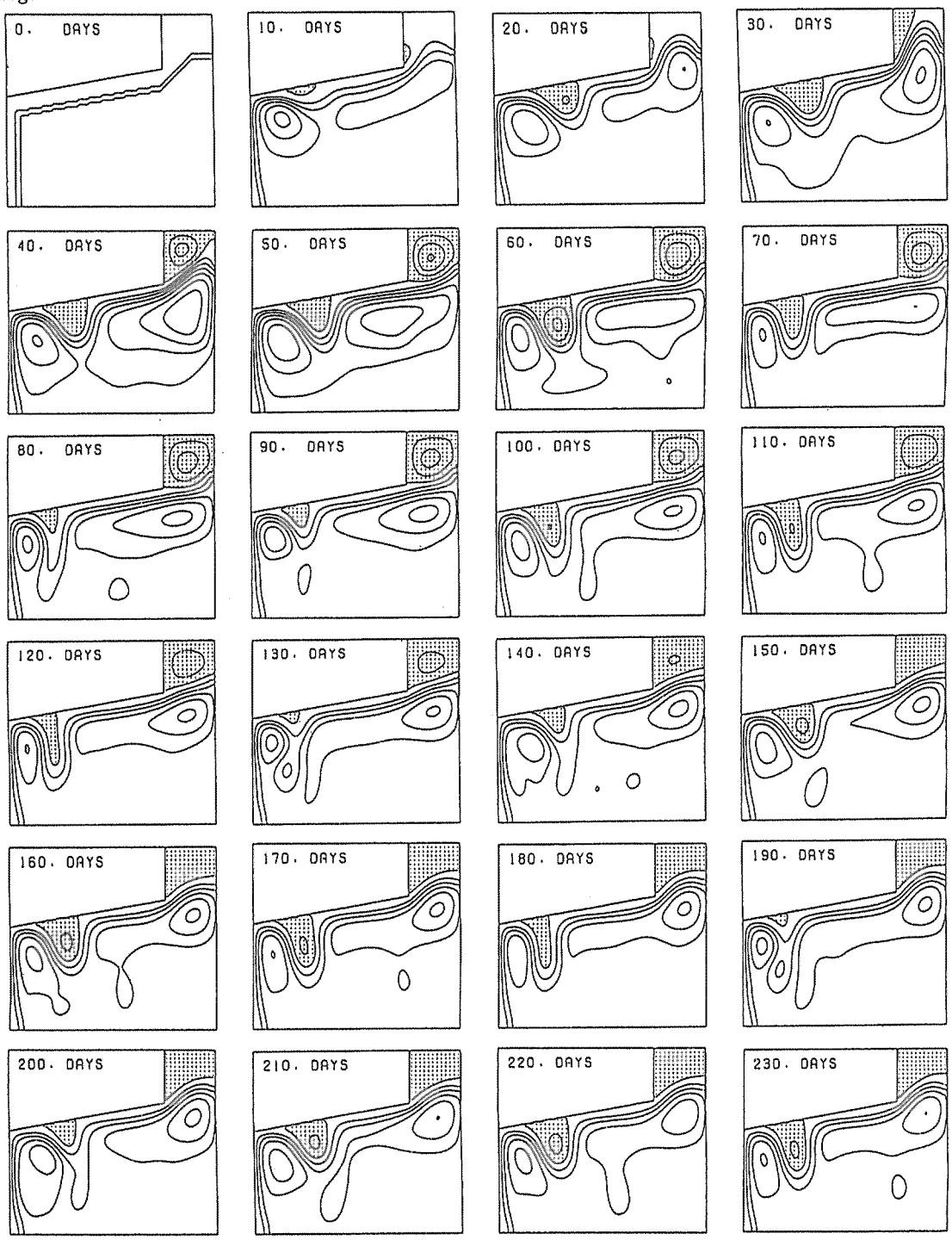

Fig. 7 Same as in Fig. 2, but for V10LE.

Fig. 7 – 2

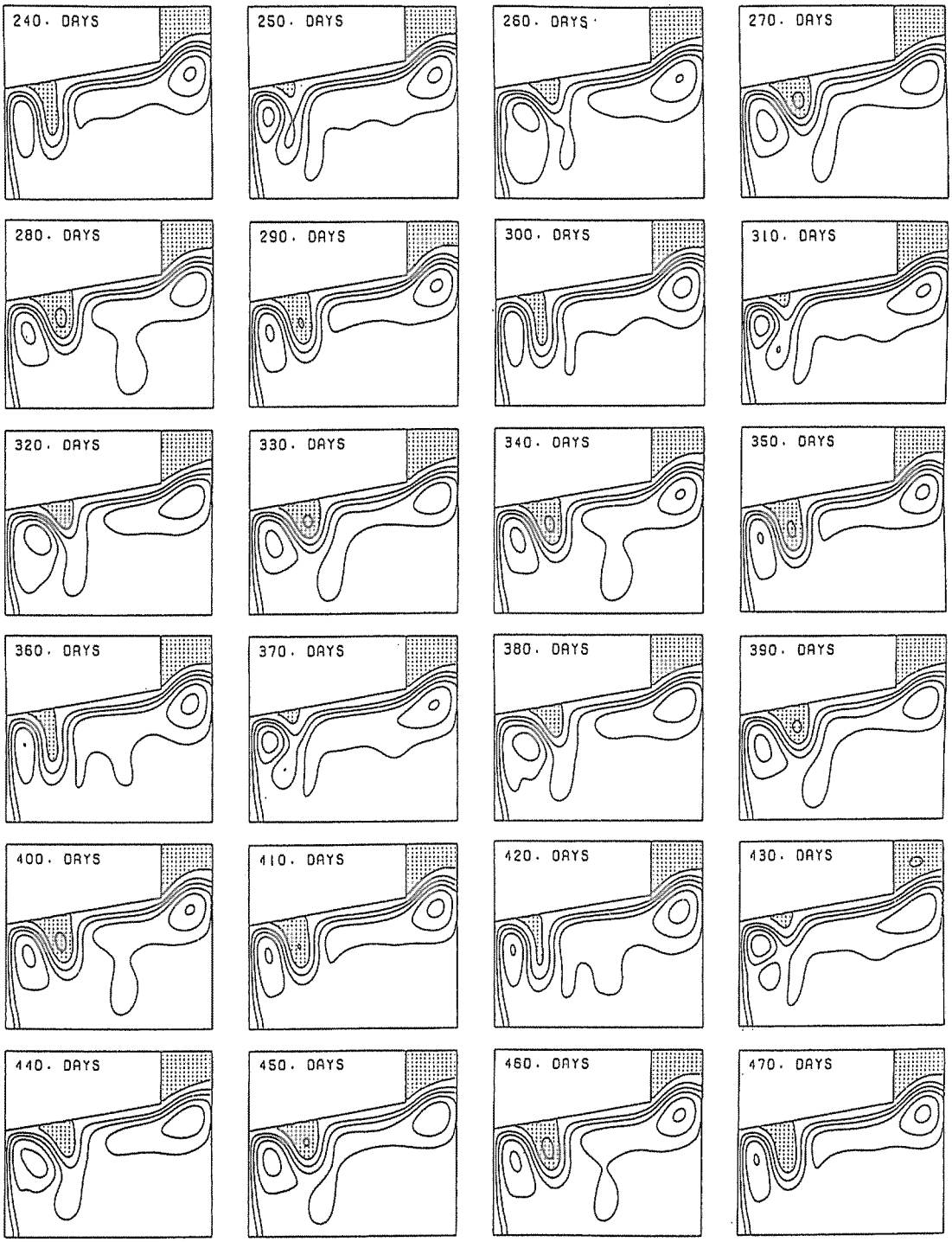
240. DAYS
250. DAYS
260. DAYS
270. DAYS
280. DAYS
290. DAYS
300. DAYS
310. DAYS
320. DAYS
330. DAYS
340. DAYS
350. DAYS
360. DAYS
370. DAYS
380. DAYS
390. DAYS
400. DAYS
410. DAYS
420. DAYS
430. DAYS
440. DAYS
450. DAYS
460. DAYS
470. DAYS

Fig. 8 – 1

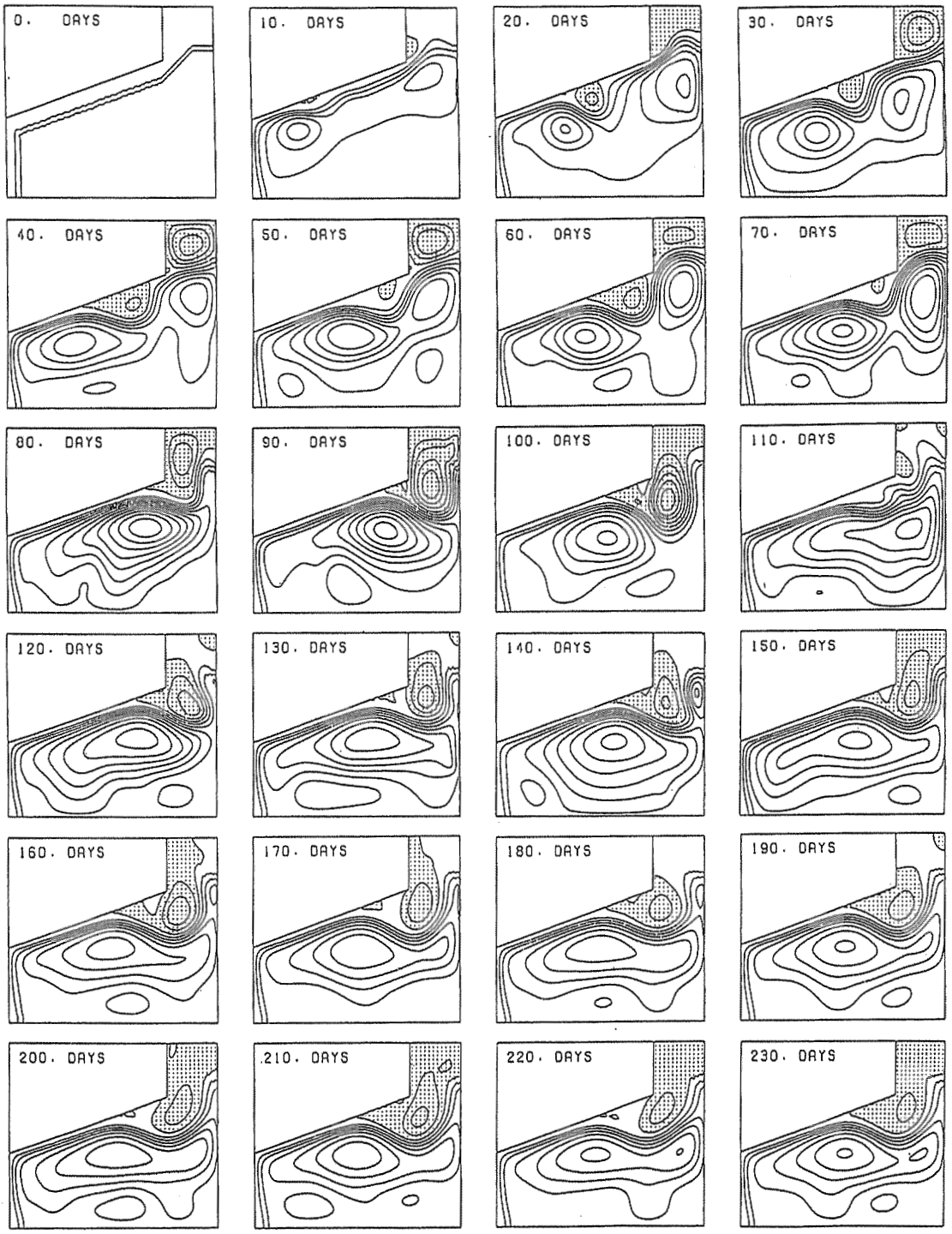

Fig. 8 Same as in Fig. 2, but for V20SE.

Fig. 8 – 2

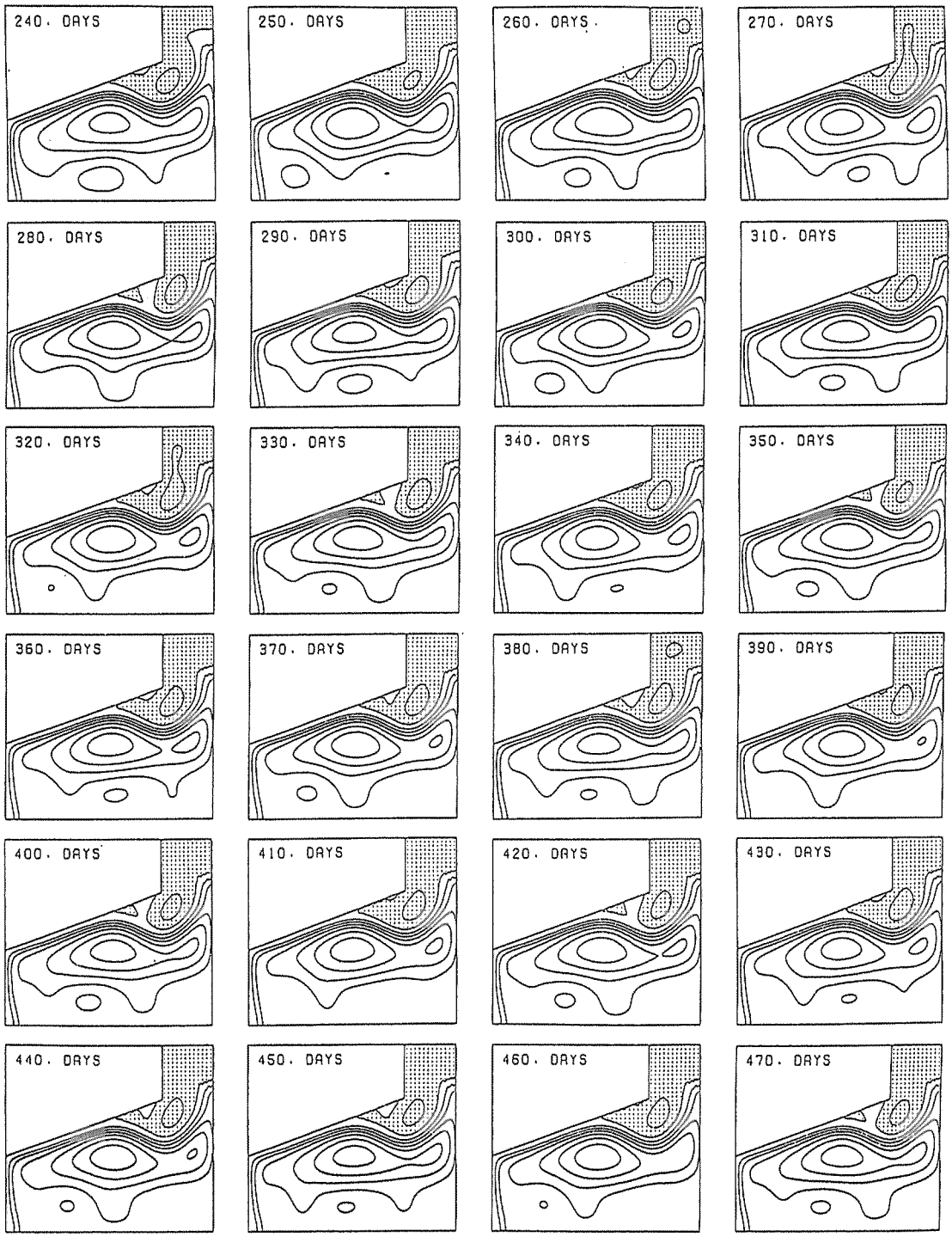
240. DAYS
250. DAYS
260. DAYS
270. DAYS
280. DAYS
290. DAYS
300. DAYS
310. DAYS
320. DAYS
330. DAYS
340. DAYS
350. DAYS
360. DAYS
370. DAYS
380. DAYS
390. DAYS
400. DAYS
410. DAYS
420. DAYS
430. DAYS
440. DAYS
450. DAYS
460. DAYS
470. DAYS

Fig. 9 – 1

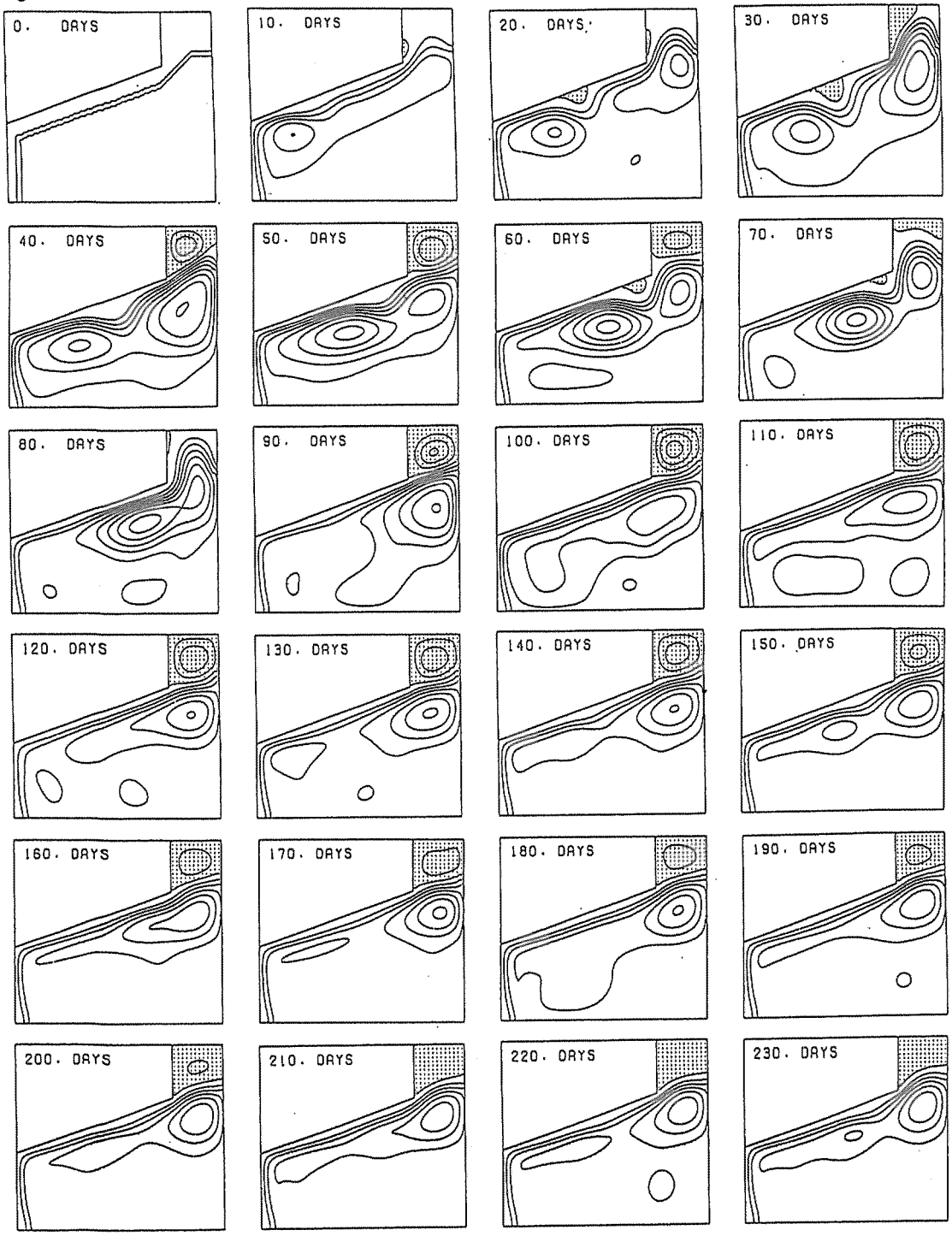

Fig. 9 Same as in Fig. 2, but for V20LE.

Fig. 9 – 2

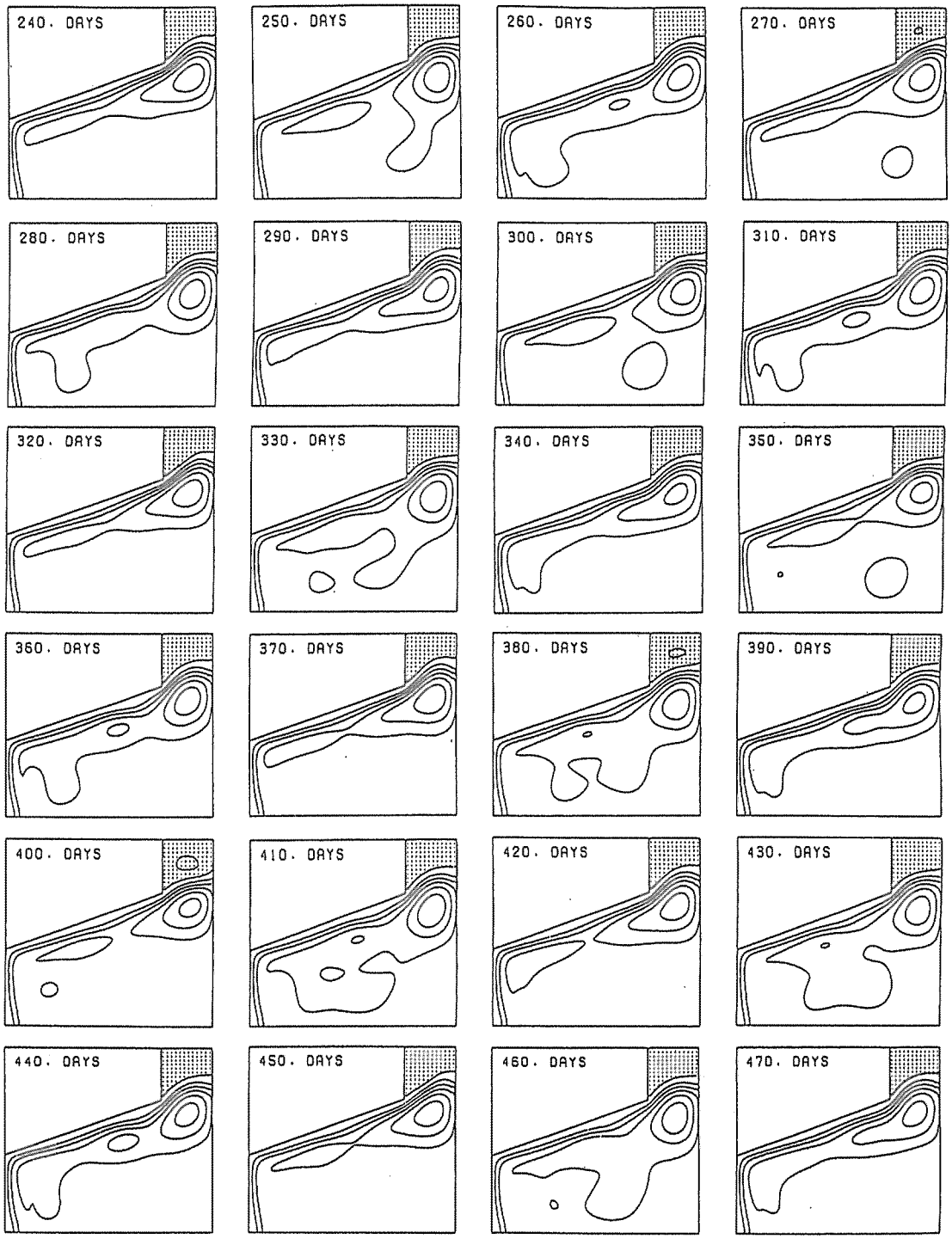
240. DAYS
250. DAYS
260. DAYS
270. DAYS
280. DAYS
290. DAYS
300. DAYS
310. DAYS
320. DAYS
330. DAYS
340. DAYS
350. DAYS
360. DAYS
370. DAYS
380. DAYS
390. DAYS
400. DAYS
410. DAYS
420. DAYS
430. DAYS
440. DAYS
450. DAYS
460. DAYS
470. DAYS

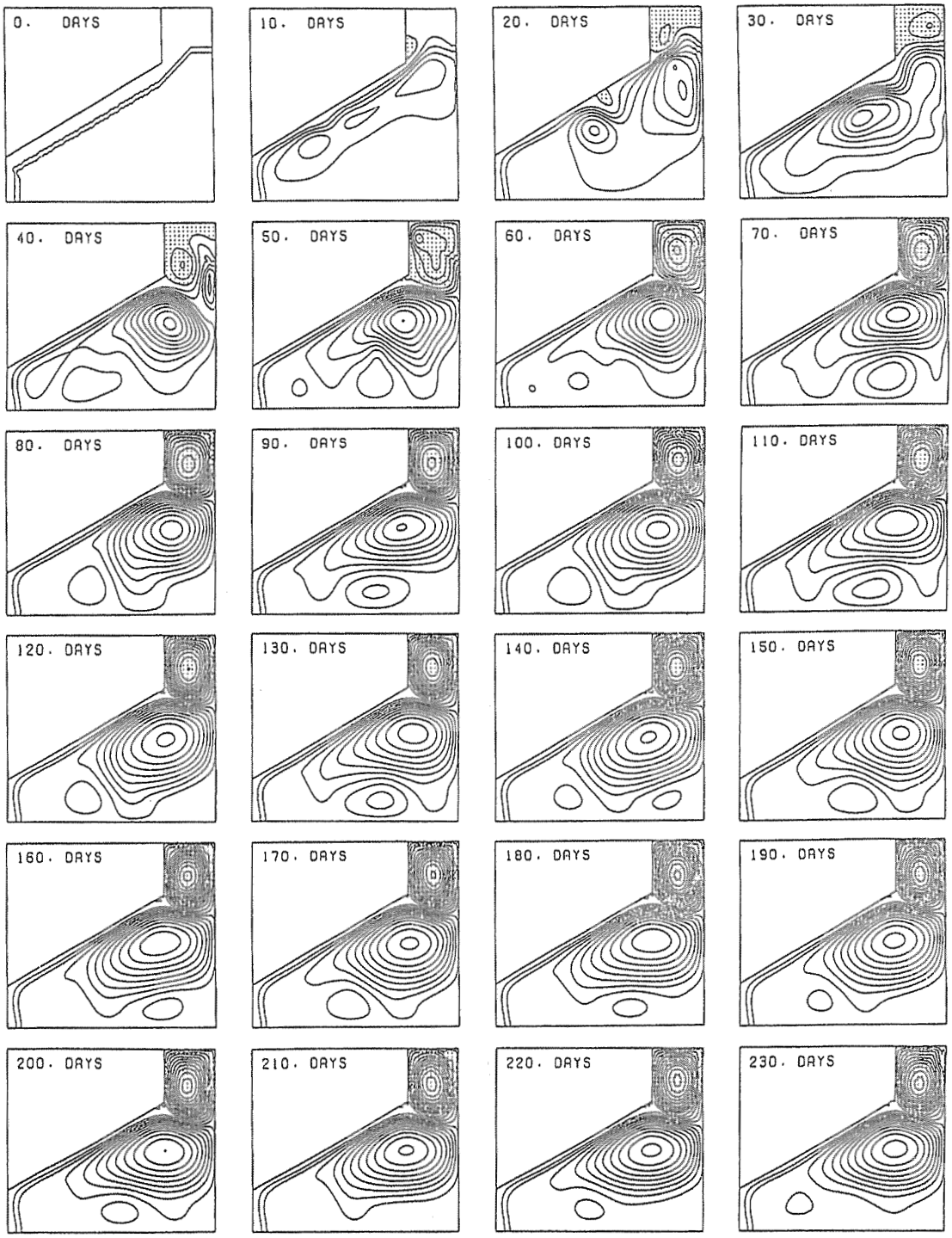

Fig. 10 Same as in Fig. 2, but for V30SE.

carried out. Although there exist weak time variations in the cyclonic eddy in north of the outflow (Fig. 5c) and in the dominant anti-cyclonic circulation shown by the contour of volume transport function lager than 60 Sv, total flow pattern attains stationary state after 120 days.

3 − 4 Cases with inclined northern boundary ($\theta = 30°$)

Results of V30SE (Fig. 10) is characterized by no formation of the cyclonic eddy in south to the inclined northern boundary. In contrast to this, cyclonic eddy in north of the mean outflow develops significantly. Stationary state is attained at about 60 - 70 days, except for the westward propagations of eddies in a southern area of the model basin. Because of the formation of large and strong anti-cyclonic flow, south-westward development of the cyclonic flow is suppressed. Totally, mean flow shows a strong tendency to flow along northern boundary. This tendency is also found in the flow pattern of V30LE (Fig. 11). However, development of the cyclonic eddy is very weak in comparison with V30 SE. Nevertheless, relatively large volume transport of the cyclonic eddy north of the mean flow is detected in an initial stage. To see the details of the variation in the cyclonic eddy in north of the mean flow, time change in the volume transport of the cyclononic eddy is shown in Fig. 12. As for V30SE, very large volume transport with irregular time change around 210 Sv is detected, while clear oscillation of the volume transport is found in V30LE, after the spin-up in the initial period. Because of the small frictional dumping in V30SE, it is indicated that enhanced cyclonic and anti-cyclonic circulation are formed by the total kinetic energy balance of the in- and outflow system.

4. Summary

The western boundary current flowing along an zonally aslant coast is examined with special reference to the degree of the coastal line inclination from zonal direction at the eastward flowing portion. As the preliminary study, basic numerical solutions have been presented. Main results of the numerical solutions are summarized as follows:

(1) It it shown from the total features of the numerical experiments that there exist two representative flow pattern: one is a mender flow pattern and the other is a straight flow pattern along northern boundary. In case of the meander flow pattern, spin-up and spin-down of the cyclonic eddy accompanied by the meander flow are carried out.

(2) Meander flow pattern is formed in the cases of zonal northern boundary. The spin-up and spin-down of the cyclonic eddy accompanied by the meander path occurs with a period of 70 days in small eddy viscosity ($A_h = 5\times10^6\ cm^2sec^{-1}$) and 50 days in larger eddy viscosity ($A_h = 10^7\ cm^2sec^{-1}$).

(3) Chaotic change from meander flow pattern to straight flow pattern occurs at about 600 days in the case V10SE with the inclination of northern boundary of 10° and small eddy viscosity. Straight mean flow along northern boundary is formed in the cases with the inclination of the northern boundary larger than 20° .

All the above results almost agree with those of Sekine[12]. However, it is shown that the cyclonic eddy formed in north of the mean outflow has a influence on the flow pattern. This cyclonic eddy is not formed in Sekine[12], in which meridional coastal boundary in the outflow area was not modeled. Because such a meridional coastal topography is common to the representative western boundary

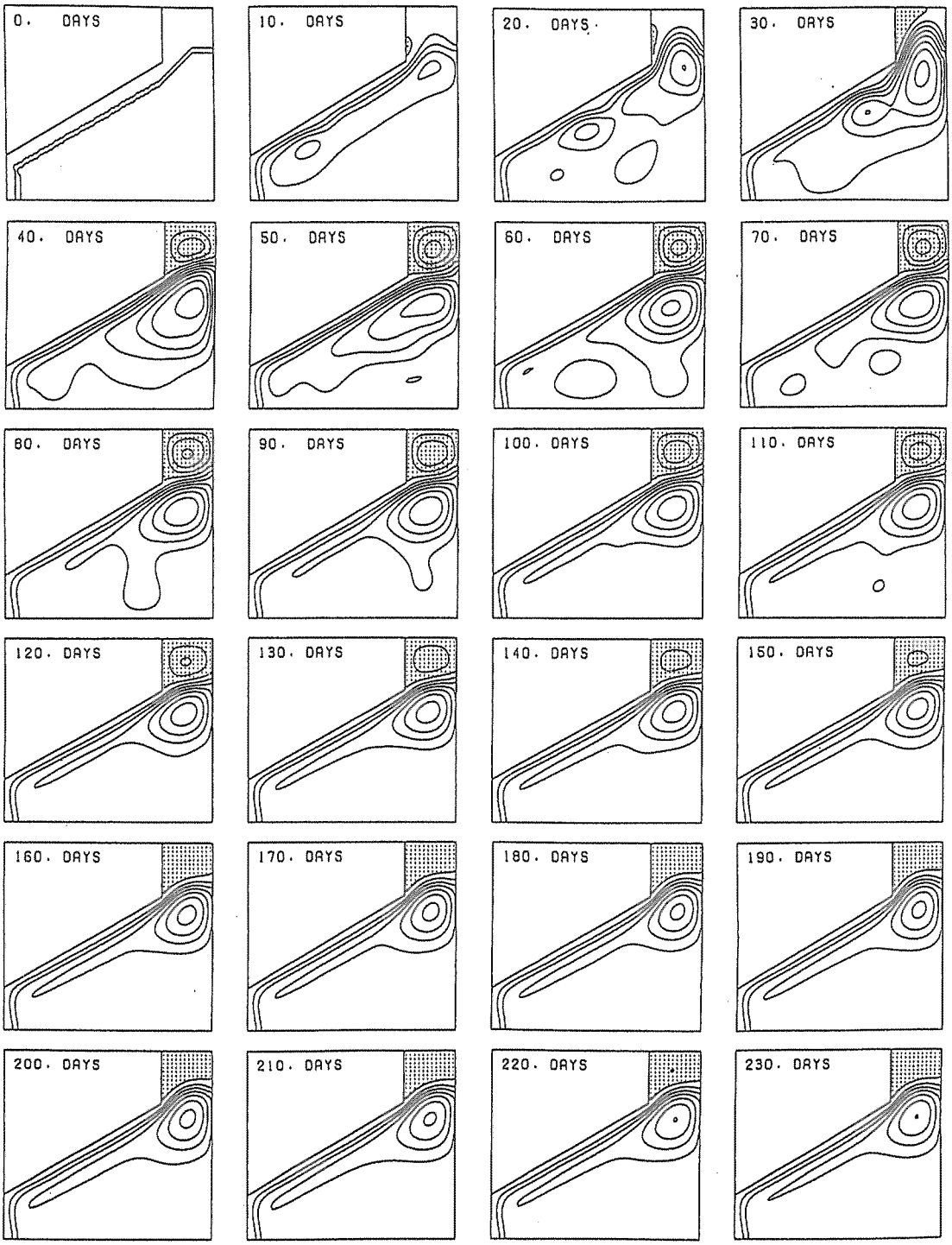

Fig. 11 Same as in Fig. 2, but for V30LE.

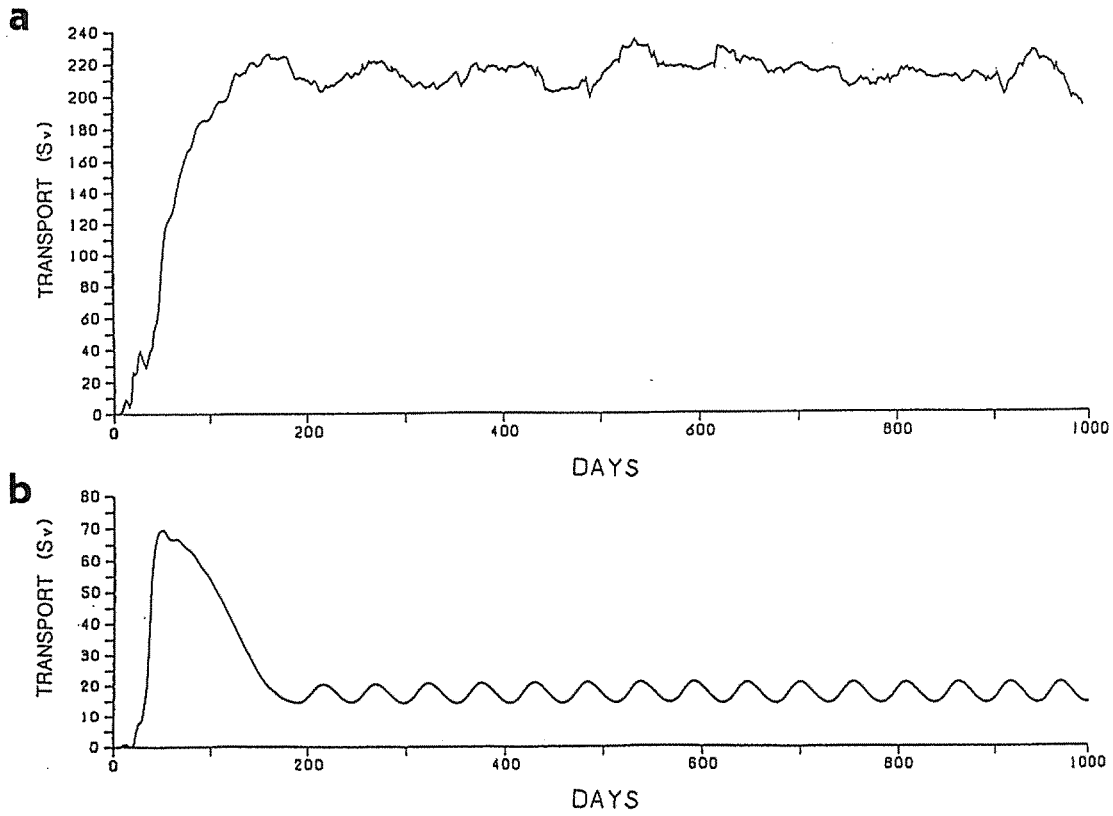

Fig. 12 Time change in the volume transport of the cyclonic eddy in northern side of the mean flow in the outflow area. (a) V30SE and (b) V30LE.

current: eastern area of Japan for the Kuroshio and northern coastal topography from Cape Hatteras for the Gulf-Stream. On the basis of these results, topographic effect of peninsula will be examined in the next step of this study.

Acknowledgment: The authors wish to express their heartfelt thanks to Prof. Y. Nagata for his valuable comment on the first manuscript. The numerical calculations were carried out on a VP- 2600 of Nagoya University and on a FACOM M- 760 of Mie University. This study was supported by a Graind in Aid for Scientific Research from the Ministry of Education, Science of Culture of Japan (05640475).

References

1) Taft, B.A. Characteristics of the flow of the Kuroshio south of Japan. In: Kuroshio - Its physical aspects, H. Stommel and K. Yoshida, editors, Univ. Tokyo press, pp.165-214 (1972).

2) Nitani, H. Variation of the Kuroshio south of Japan. J. Oceanogr. Soc. Japan, 31, 154-173 (1975).

3) Ishii, H., Y. Sekine and Y. Toba. Hydrographic structure of the Kuroshio large meander-cold water mass region down to the deeper layers of the ocean. J. Oceanogr. Soc. Japan, 39, 240-250

(1983).
4) Robinson, A. The Gulf Stream, Phil. Trans. R. Soc. Lond. A., **270**, 351-370 (1971).
5) White, W.B. and J.P. McCreary. The Kuroshio meander and its relationship to the large-scale ocean circulation. Deep-Sea Res., **23**, 33-47 (1976).
6) Chao,S-Y. and J.P. McCreary. A numerical study of the Kuroshio south of Japan. J. Phys. Oceanogr., **12**, 680-693 (1982).
7) Masuda, A. An interpretation of the bimodel character of the stable Kuroshio path. Deep-Sea Res., **29**, 471-484 (1982).
8) Yasuda, I. J.H. Yoon and N. Suginohara. Dynamics of the Kuroshio large meander-barotropic model. J. Oceanogr. Soc. Japan, **41**, 259-273 (1985).
9) Chao, S-Y. Bimodality of the Kuroshio. J. Phys. Oceanogr., **14**, 92-103 (1984).
10) Yamagata, T. and S. Umatani. Geometry-forced coherent structure as a model of the Kuroshio large meander. J. Phys. Oceanogr., **19**, 130-138 (1989).
11) Yoon, J. H. and I. Yasuda. Dynamics of the Kuroshio large meander. Two-layer model. J. Phys. Oceanogr., **17**, 66-81 (1987).
12) Sekine, Y. Coastal and bottom topographic effects on the path dynamics of the western boundary current with special reference to the Kuroshio south of Japan. La mer, **26**, 99-144 (1988).
13) Sekine, Y. A numerical experiment on the path dynamics of the Kuroshio with reference to the formation of the large meander path south of Japan. Deep-Sea Res., **37**, 359-380 (1990).
14) Akitomo, K., T. Awaji and N. Imasato. Kuroshio path variation south of Japan. 1 Barotropic inflow-outflow model. J. Geophys. Res., **96**, 2549-2560 (1991).

西岸境界流に及ぼす陸岸地形効果

第1部　陸岸地形の東西からの傾きの影響

関根　義彦・麻生　晃也
三重大学生物資源学部

要旨：順圧数値モデルを用いて西岸境界流に及ぼす陸岸地形効果に関して，特に東西方向からの北側陸岸境界の傾斜の影響を調べた。この論文では得られた結果の詳細な流れのパターンを提示した。数値モデル実験により，蛇行する流れのパターンと岸に沿う直進する流れのパターンの二つの代表的なパターンがあることが示された。蛇行する流れのパターンの場合には，蛇行する一般流に伴い低気圧渦が生じ，強化と減衰を繰り返す。蛇行パターンは北側の境界が東西の場合に生じる。カオス的な蛇行パターンから直進パターンへの変化が10°の東西方向からの傾斜と相対的に小さい渦粘性係数を与えたモデルで発生した。直進する一般流は東西方向からの傾斜が大きい場合に発生する傾向が見られた。